Liquid Crystals
Publication details, including instructions for authors and subscription information:
http://www.informaworld.com/smpp/title~content=t713926090

Tailoring of ionic supramolecular assemblies based on ammonium carboxylates toward liquid-crystalline micellar cubic mesophases

Takao Noguchi[a]; Keiki Kishikawa[b]; Shigeo Kohmoto[b]
[a] Quality Materials Science, Graduate School of Science and Technology, Chiba University, Chiba 263-8522, Japan [b] Department of Applied Chemistry and Biotechnology, Graduate School of Engineering, Chiba University, Chiba 263-8522, Japan

To cite this Article Noguchi, Takao , Kishikawa, Keiki and Kohmoto, Shigeo(2008) 'Tailoring of ionic supramolecular assemblies based on ammonium carboxylates toward liquid-crystalline micellar cubic mesophases', Liquid Crystals, 35: 8, 1043 — 1050
To link to this Article: DOI: 10.1080/02678290802364343
URL: http://dx.doi.org/10.1080/02678290802364343

Liquid Crystals,
Vol. 35, No. 8, August 2008, 1043–1050

Taylor & Francis
Taylor & Francis Group

Tailoring of ionic supramolecular assemblies based on ammonium carboxylates toward liquid-crystalline micellar cubic mesophases

Takao Noguchi[a], Keiki Kishikawa[b] and Shigeo Kohmoto[b]*

[a]*Quality Materials Science, Graduate School of Science and Technology, Chiba University, 1-33 Yayoi-choInage-ku, Chiba 263-8522, Japan;* [b]*Department of Applied Chemistry and Biotechnology, Graduate School of Engineering, Chiba University, 1-33 Yayoi-cho, Inage-ku, Chiba 263-8522, Japan*

(Received 28 March 2008; final form 23 July 2008)

Ionic liquid crystals based on ionic complexation of tris(2-aminoethyl)amine (**1**) with 3,4,5-tris(7,7,8,8,9,9,10,10,11,11,12,12,12-tridecafluorododecyloxy)benzoic acid (**2**) and with 3,4,5-tris(2-octyldodecyloxy)benzoic acid (**3**) were investigated. The ionic complex with the partially fluorinated alkyl chains (**1**·**2**) exhibited a morphological transition from a hexagonal columnar mesophase to a *Pm*3*n* micellar cubic phase upon increasing the molar ratio of **2** to **1**. For the complex with the branched alkyl chains (**1**·**3**) a micellar cubic mesophase was exclusively generated at appropriate composite ratios. The generation of the micellar cubic mesophases is attributed to the introduction of the laterally expanded volume of the alkyl chains compared with the corresponding normal dodecyl chains. Their thermal stabilities were most enhanced at a specific molar ratio of 1:5 for **1**·**2** and 1:4 for **1**·**3**. This result corresponds to the most suitable chain volume for the stable micellar cubic mesophase.

Keywords: cubic mesophase; ammonium carboxylates; ionic interaction; microsegregation

1. Introduction

The investigation of morphological diversification by using a simple molecular or supramolecular system is of importance to obtain profound insights into structural design toward the tailoring of mesomorphic superstructures. The morphologies of the thermotropic liquid crystalline (LC) phases are tailored mainly by molecular or supramolecular shapes. The main LC phases, i.e. smectic and columnar phases, are observed depending on the rod-like and disc-like shapes, respectively, of the constituting molecules (*1*). Such molecules can even exhibit different types of thermotropic LC phases, i.e. bicontinuous cubic mesophases (*2–7*). On the other hand, thermotropic micellar cubic mesophases have been found for amphiphilic and dendritic molecules (*8–15*). It has recently been reported that amphiphilic molecules possessing polyhydroxy/aliphatic chain subunits exhibit a wide variety of thermotropic LC mesophases in a phase sequence of lamellar, bicontinuous cubic, columnar and micellar cubic (*16*). The type of phase can be controlled simply by varying the length and/or the number of aliphatic chains and hydroxyl groups. The driving force for their occurrence is microsegregation, which requires distinct spaces to accommodate each incompatible molecular subunit (*17*). The changeability of the curvature of the interface dividing the subspace is responsible for their morphological diversity. Such morphological studies of mesophases have recently been examined for supramolecular LC systems incorporating triazine/benzoic acid (*18, 19*). In these supramolecular systems, the composite ratio of the constituting building blocks becomes an additional parameter to determine the interface geometry of molecular aggregates.

We have been interested in the tailoring of LC ionic complexes comprised of different molecular building blocks via ionic interactions. A significant amphiphilicity can be induced upon ionic complexation. The amphiphilicity with which ionic liquid crystals are endowed is a considerable feature (*20–28*). We have recently reported ionic liquid crystals based on ammonium carboxylates composed of tris(2-aminoethyl)amine (**1**, figure 1) and alkoxy-substituted benzoic acids. The suitable interfacial curvature of the ionic complex of **1** and 3,4-dioctyloxybenzoic acid for smectic A and hexagonal columnar phases can be adjusted by controlling the composite ratio of the acid to **1**, i.e. the volumetric ratio of the alkyl chains in the resulting ionic complexes introduced by the acid (*29*). We have pointed out that the best volumetric balance for the most thermally stable columnar mesophase is attained with a particular packing fraction of the ionic complexes against its unit cell (*30*).

*Corresponding author. Email: kohmoto@faculty.chiba-u.jp

ISSN 0267-8292 print/ISSN 1366-5855 online

DOI: 10.1080/02678290802364343
http://www.informaworld.com

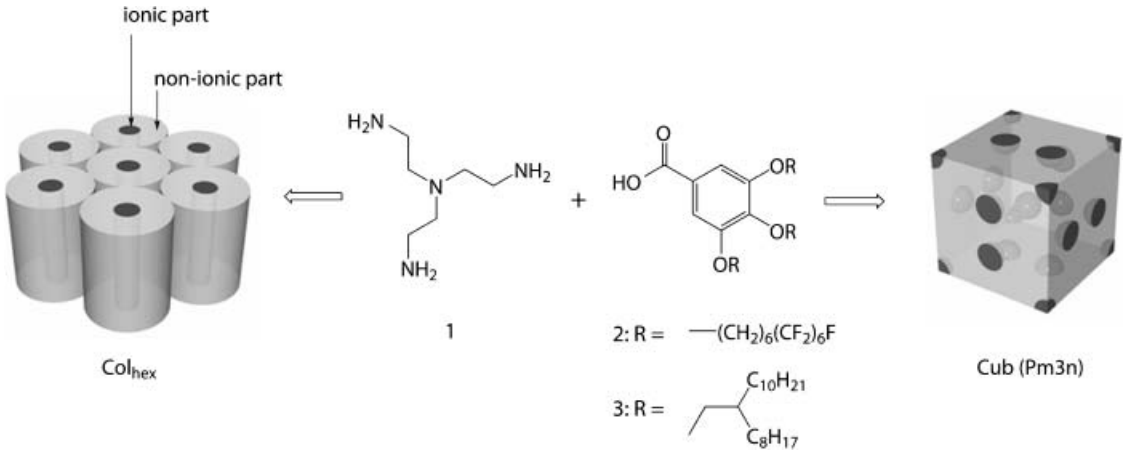

Figure 1. Chemical structures of amine (**1**) and acids (**2** and **3**), and schematic illustration of a hexagonal columnar and *Pm*3*n* micellar cubic mesophases.

In this paper, we report on micellar cubic mesophases built up by binary ionic complexes composed of tris(2-aminoethyl)amine (**1**) and 3,4,5-trialkoxybenzoic acids with partially fluorinated alkyl chains (**2**) and with branched alkyl chains (**3**) (figure 1). Toward the diversification of mesophase morphology formed by these ionic complexes, an incremental approach to increase the chain volume of the acids could be promising for the generation of cubic mesophases. The introduction of fluorinated alkyl chains into a LC system was expected to modify mesomorphic properties (including mesophase morphologies and thermal stabilities) owing not only to their stiffness and incompatibility but also to their larger cross-sectional area, compared to normal alkyl chains (*13–15*, *31–36*). Ionic complex **1**·**2** exhibited a morphological transition from a hexagonal columnar (Col_{hex}) mesophase to a *Pm*3*n* micellar cubic (Cub) upon increasing the molar ratio of the acid to the amine, whereas a complex with the corresponding dodecyl alkyl chains exclusively exhibited a hexagonal columnar mesophase (*30*). Complex **1**·**3** with branched alkyl chains seems to be unfavourable for the mesophase formation owing to their sterical overcrowding. However, they supply an appropriate chain volume enough to stabilise spheroidic aggregates toward the formation of a micellar cubic mesophase.

2. Experimental

General methods and materials

^{1}H NMR (500 MHz) and ^{13}C NMR (125 MHz) spectra were recorded on a JEOL LA500 spectrometer. Chemical shifts are reported in ppm with the signals of TMS for ^{1}H NMR spectra and solvents for ^{13}C NMR spectra used as internal standards. IR spectra were recorded on a JASCO FT/IR410 spectrometer. High-resolution mass spectra were recorded using a JEOL JMS-HX110 instrument. Thermal transitions of the ionic complexes were investigated by differential scanning calorimetry (DSC) using a MAC Science DSC3100S differential scanning calorimeter and heating and cooling rates of $5^\circ C\,min^{-1}$. Using a Nikon Eclipse E400POL equipped with an Instec HCS400 hot stage, polarising optical microscopy (POM) was used to verify thermal transitions and characterise anisotropic textures. X-ray diffraction (XRD) experiments were performed with Cu K_α radiation by using a Rigaku RINT 2200 diffractometer.

All commercially available chemicals and solvents were of reagent grade and used as received without further purification. The benzoic acid with partially fluorinated alkyl chains (**2**) is a known compound and was synthesised by the reported method (*36*). Scheme 1 shows the synthesis of the novel benzoic

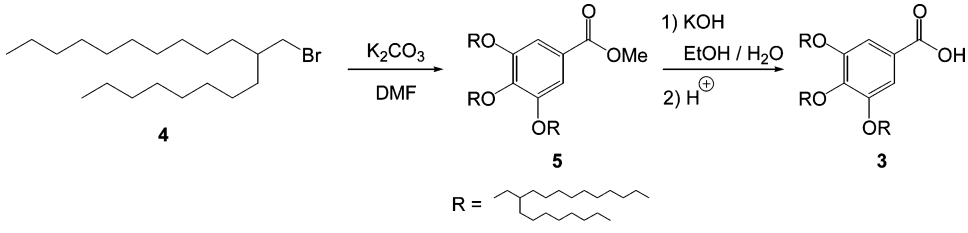

Scheme 1. Synthetic route to acid **3**.

acid with branched alkyl chains (**3**). 1-Bromo-2-octyldodecane **4** is a known compound and was synthesised according to the reported procedure (*37*).

Synthesis

*Methyl 3,4,5-tris(2-octyl-dodecyloxy)benzoate (**5**).*

Compound **4** (3.32 g, 9.19 mmol) was added to a mixture of methyl 3,4,5-trihydroxybenzoate (423 mg, 2.30 mmol) and K_2CO_3 (1.90 g, 13.7 mmol) in dry DMF (15 ml) under Ar. The reaction mixture was stirred at 70°C for 18 h under Ar, and then it was cooled to room temperature. The reaction mixture was dissolved in ethyl acetate, and washed three times with H_2O and once with brine. The organic phase was dried over anhydrous $MgSO_4$ and concentrated to dryness. The crude product was purified by column chromatography on silica gel. Hexane was used as an eluent to remove excess amount of bromide **4** followed by elution with hexane/ethyl acetate 99:1 to give **5** as a colourless liquid (2.01 g, 85% yield). ^{1}H NMR (500 MHz, $CDCl_3$): δ 0.88 (t, J=6.4 Hz, 18H), 1.26–1.55 (m, 96H), 1.74 (m, J=5.8 Hz, 1H), 1.80 (m, J=5.8 Hz, 2H), 3.87 (d, J=5.8 Hz, 4H), 3.88 (d, J=5.8 Hz, 2H), 3.89 (s, 3H), 7.24 (s, 2H). ^{13}C NMR (125 MHz, $CDCl_3$): δ 14.1, 22.7, 26.9, 27.1, 29.37, 29.42, 29.47, 29.67, 29.73, 29.77, 29.82, 30.1, 30.2, 31.2, 31.4, 31.93, 31.96, 31.97, 38.2, 39.3, 52.1, 71.5, 76.4, 107.4, 124.4, 142.4, 153.0, 167.1. IR (neat, cm^{-1}): 2924, 2854, 1724, 1588, 1432, 1335, 1215. HRMS (FAB, m/z): calculated for $C_{68}H_{129}O_5$ $[M+H]^+$, 1025.9840; found, 1025.9866.

*3,4,5-Tris(2-octyl-dodecyloxy)benzoic acid (**3**).*

A mixture of compound **5** (2.01 g, 1.96 mmol), EtOH (30 ml), H_2O (3 ml) and KOH (510 mg, 9.09 mmol) was heated under reflux for 2 h while stirring. The reaction mixture was cooled to room temperature, acidified with 10% aq. HCl to pH 1 and evaporated to remove EtOH. The resulting mixture was extracted with $CHCl_3$. The organic phase was dried over anhydrous $MgSO_4$ and concentrated to dryness. The crude product was purified by column chromatography on silica gel (hexane/ethyl acetate 10:1) to give **3** as a colourless liquid (1.70 g, 86% yield). ^{1}H NMR (500 MHz, $CDCl_3$): δ 0.88 (t, J=5.8 Hz, 18H), 1.26–1.57 (m, 96H), 1.75 (m, J=5.8 Hz, 1H), 1.81 (m, J=5.8 Hz, 2H), 3.89 (d, J=5.8 Hz, 4H), 3.92 (d, J=5.8 Hz, 2H), 7.32 (s, 2H). ^{13}C NMR (125 MHz, $CDCl_3$): δ 14.12, 22.72, 22.74, 26.9, 27.1, 29.40, 29.42, 29.45, 29.50, 29.70, 29.74, 29.76, 29.79, 29.9, 30.1, 30.3, 31.3, 31.4, 31.96, 31.99, 32.01, 38.2, 39.3, 71.6, 76.5, 108.1, 123.4, 143.3, 153.0, 171.9. IR (neat, cm^{-1}): 2923, 2853, 1685, 1585, 1430, 1328, 1227, 1114. HRMS (FAB, m/z): calculated for $C_{67}H_{126}O_5$ $[M]^+$, 1010.9605; found, 1010.9584.

Preparation of ionic complexes.

The ionic complexes **1·2** and **1·3** were obtained as colourless solids by mixing **1** and **2**–**3** in chloroform with appropriate molar ratios followed by evaporation of the solvent. The occurrence of the ionic complexation was confirmed by FT-IR measurements, which showed the carboxylate (COO^-) absorption bands at 1543 cm^{-1} (ν_{as}) and 1379 cm^{-1} (ν_s).

3. Results and discussion

General trends

The effect of the amine–acid composite ratio on mesomorphic properties of the resulting ionic complex was examined. The phase behaviours of the ionic complexes were investigated by DSC and POM. Figure 2 shows phase diagrams as a function of the molar ratio of the acids to **1**. The observed mesophases (Col_{hex} and Cub) and their thermal stabilities were strongly dependent on the amine–acid ratios. On POM investigation typical spherulitic textures were appeared in their Col_{hex} phases. On the other hand, optically isotropic textures with high viscosity were observed in their Cub phases. The highest clearing temperature of mesophase (the thermally most stable mesophase) was observed at a particular molar ratio specific to the mesophase morphology. The phase behaviours of the ionic complexes at the most suitable molar ratio and their XRD results are summarised in Tables 1 and 2, respectively.

Mesomorphic properties of complex 1·2

Complex **1·2** bearing partially fluorinated alkyl chains showed ratio-dependent organisation of a Col_{hex} and cubic mesophases. Phase diagrams are shown in Figure 2(a). Their thermal stabilities were most enhanced at the molar ratios of 1:1.3 for the Col_{hex} and 1:5 for the cubic mesophases. For the complex at the ratio of 1:1.3, spherulitic textures were observed on POM investigation (Figure 3(a)). XRD measurements on the mesophase at 105°C revealed three reflections in the small-angle region with d-spacings in the reciprocal ratio of 1:$\sqrt{3}$:$\sqrt{4}$ (Figure 3(b)). These were indexed as (100), (110) and (200) reflections, respectively, of a two-dimensional (2D) hexagonal lattice with a lattice constant a_{hex}=35.5 Å. A broad halo was also observed in the wide-angle region around 5.4 Å corresponding to the mean distance between the partially fluorinated alkyl chains. The observed lattice

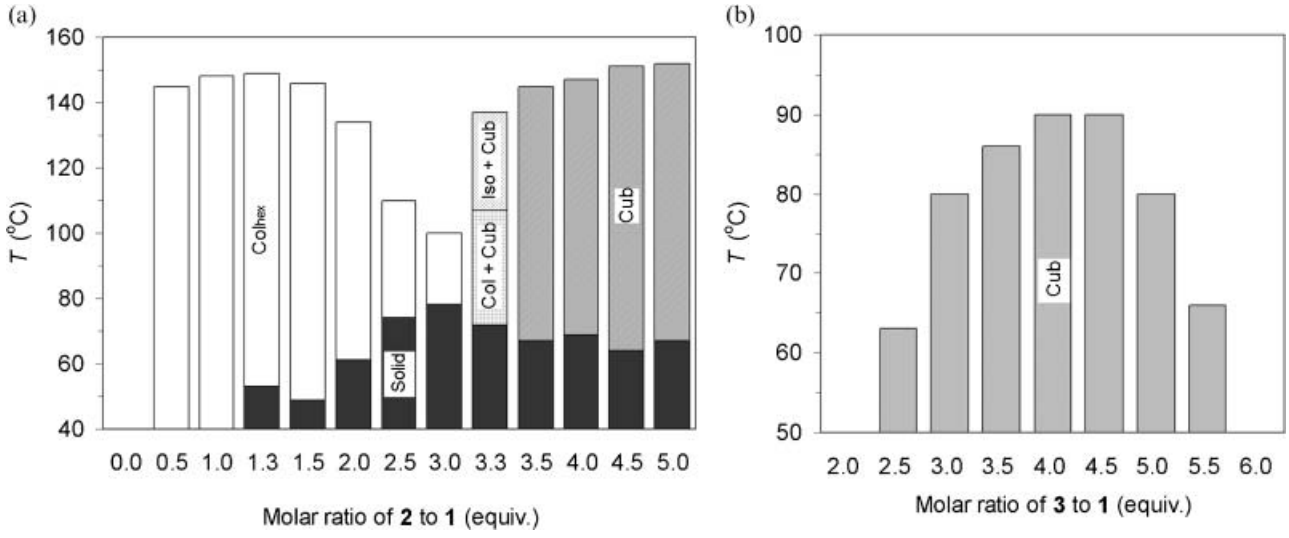

Figure 2. Phase diagrams of ionic complexes (a) **1·2** (b) **1·3**.

constant (a_{hex}) is approximately 80% of the calculated column diameter (D) with the assumption of fully extended alkyl chains (a_{hex}/D=0.78). This is often observed for columnar mesophases owing to the disordered conformation of the alkyl chains and some degree of their interdigitation between the columnar aggregates. In the Col_{hex} phase, a column is comprised of polymolecular cylindrical aggregates where the partially ionized **1** is surrounded by the ionized acid **2**. Because of a non-stoichiometric complex of amine and acid in the Col_{hex} phase, non-ionized free amino groups could participate in ionic hydrogen bonds with charged species such as NH_3^+ and COO^- (*38, 39*). In this study, however, these types of interactions were hardly detected in FT-IR measurements.

The thermally most stable Col_{hex} phase was found at the particular molar ratio of 1:1.3 for the complex **1·2**, whereas the complex with its non-fluorinated analogue showed the most suitable ratio of 1:2 (*30*). The difference in these ratios for the Col_{hex} phases could be the result of the volumetric adjustment of the peripheral chain part for the formation of the ideal columnar aggregates. Since the cross-sectional area of the fluorinated chain (ca. 30 Å^2) is ca. 1.5 times larger than that of the alkyl chain (ca. 20 Å^2) (*14, 18, 40*), the most suitable ratio of **1·2** (1:1.3) for the Col_{hex} phase is deduced to be about two-thirds of

Table 1. Phase transition behaviour of the ionic complexes at the most suitable ratio.

Complex	Molar ratio	Phase transitions[a]
1·2	1:1.3	Cr 53 (3.1) Col_{hex} 149 (1.9) I
	1:5	G 67 Cub 152 (2.6) I
1·3	1:4	G –[b] Cub 89 (0.7) I

[a]Transition temperatures (°C) and the corresponding enthalpies (in parentheses, kJ mol^{-1}) were determined by DSC on the second heating scan (rate: 5°C min^{-1}). G, Cr, Col_{hex}, Cub and I indicate glassy, crystal, hexagonal columnar, *Pm3n* cubic and isotropic liquid phases, respectively. [b]Not detectable.

Table 2. XRD results and structural parameters.

Composite ratio	T /°C	d_{obs} (d_{calc}) /Å[a]	$h\ k\ l$	Mesophase and lattice constant[b]
1·3 (1:1.3)	105	30.7 (30.7)	100	Col_{hex}
		17.7 (17.7)	110	a_{hex}=35.5 Å
		15.4 (15.4)	200	a_{hex}/D=0.78
1·3 (1:5)	120	33.2 (33.3)	200	Cub (*Pm3n*)
		29.7 (29.7)	210	a_{cub}=66.5 Å
		27.1 (27.2)	211	n=3.2
		–	220	
		–	310	
		19.1 (19.2)	222	
		18.5 (18.4)	320	
		17.8 (17.8)	321	
		16.7 (16.6)	400	
		14.9 (14.9)	420	
		14.5 (14.5)	421	
1·4 (1:4)	55	28.6 (28.7)	200	Cub (*Pm3n*)
		25.7 (25.6)	210	a_{cub}=57.3 Å
		23.4 (23.4)	211	n=3.4

[a]d_{obs} and d_{calc} are the observed and calculated d-spacings on XRD, respectivery. d_{calc} is deduced from the following equation: $<d_{100}>_{hex}=(d_{100}+\sqrt{3}d_{110}+2d_{200})/3$ for the Col_{hex} phase; $<d_{100}>_{cub}=(\sqrt{4}d_{200}+\sqrt{5}d_{210}+\sqrt{6}d_{211}+\sqrt{12}d_{222}+\sqrt{13}d_{320}+\sqrt{14}d_{321}+\sqrt{16}d_{400}+\sqrt{5}d_{210}+\sqrt{6}d_{211}+\sqrt{12}d_{222}+\sqrt{13}d_{320}+\sqrt{14}d_{321}+\sqrt{16}d_{400}+\sqrt{20}d_{420}+\sqrt{21}d_{421}+\sqrt{12}d_{222}+\sqrt{13}d_{320}+\sqrt{14}d_{321}+\sqrt{16}d_{400}+\sqrt{20}d_{420}+\sqrt{21}d_{421})/9$ for the Cub (*Pm3n*) phase. [b]a_{hex} is the lattice constant of the Col_{hex} phase: $a_{hex}=2<d_{100}>_{hex}/\sqrt{3}$. a_{cub} is the lattice constant of the Cub (*Pm3n*) phase: $a_{cub}=<d_{100}>_{cub}$. D is the diameter of the column calculated by the molecular modelling. n is the number of the ionic complex at the ratio indicated in each micelle of the cubic mesophase (calculated using the equation $n=a_{cub}{}^3\rho N_A/8M_w$, where ρ is the volume mass ($\approx$1 g/cm^3), N_A is the Avogadro number, M_w is the molecular weight of the ionic complex at the composite ratio indicated).

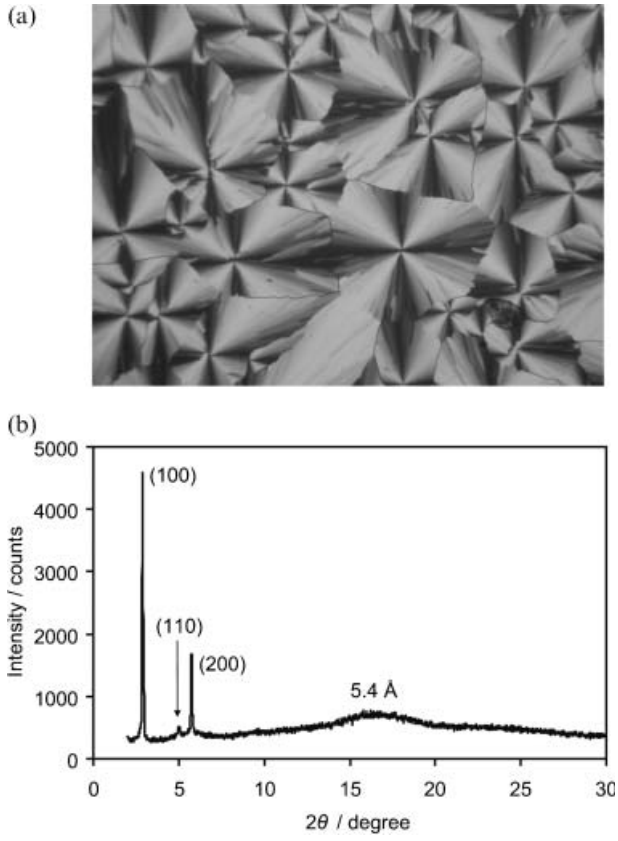

Figure 3. (a) Optical texture of the columnar phase for **1·2** (1:1.3) at 130°C. (b) XRD pattern of **1·2** (1:1.3) at 105°C.

that of the complex with its non-fluorinated analogue (1:2). This result supports our previous report (*30*) on the importance of the packing fraction of the ionic complex in a Col_{hex} phase.

An increase in the composite ratio altered the mesophase from a Col_{hex} to a cubic. The complex **1·2** with the molar ratio of 1:5 displayed an optically isotropic texture with high viscosity on POM investigation. DSC measurements indicated a clear phase transition peak from the optically isotropic mesophase to the isotropic liquid. Its XRD pattern in the mesophase at 120°C exhibited nine reflections in the small-angle region with *d*-spacings in the reciprocal ratio of $\sqrt{4}$:$\sqrt{5}$:$\sqrt{6}$:$\sqrt{12}$:$\sqrt{13}$:$\sqrt{14}$:$\sqrt{16}$:$\sqrt{20}$:$\sqrt{21}$, which were indexed as (200), (210), (211), (222), (320), (321), (400), (420) and (421) reflections, respectively (Figure 4(a)). A broad halo was also observed in the wide-angle region around 5.4 Å, indicating the LC order. The peak pattern and the phase sequence located above a hexagonal columnar phase accompanied with increasing the molar ratio of **2** indicate the generation of a three-dimensionally organised micellar cubic mesophase with *Pm*3*n* symmetry (*41–44*) with a lattice constant a_{cub}=66.5 Å. Based on the results, the number of complexes (1:5) constituting a micellar aggregate was estimated to be ≈3. This means that a micellar aggregate is constituted of a mixture of three 1:3 ionic complexes (**1·2**) and six non-ionized acid **2**, because protonation of **1** is known to occur at three primary amino groups (*45*) and actually confirmed by the FT-IR measurements. In its cubic mesophase, ionic hydrogen bonds between the non-ionized COOH and charged species could furnish the formation of appropriate micellar aggregates.

Mesomorphic properties of complex 1·3

A cubic mesophase was also observed for the complex **1·3** with branched alkyl chains. It dominantly showed a cubic mesophase and most stabilised at the ratio 1:4 (Figure 2(b)). On POM investigation, the formation of a highly viscous and optically isotropic texture was confirmed. XRD measurements in the mesophase at 55°C showed three reflections in the small-angle region with *d*-spacings in the reciprocal ratio of $\sqrt{4}$:$\sqrt{5}$:$\sqrt{6}$, which were indexed as (200), (210) and (211) reflections, respectively (Figure 4(b)). A broad halo was also observed in the wide-angle region around 4.5 Å corresponding to the conformational disorder of the alkyl chains. The distribution of the intensities and *d*-spacings together with the POM observation indicate the generation of a three-dimensionally organised

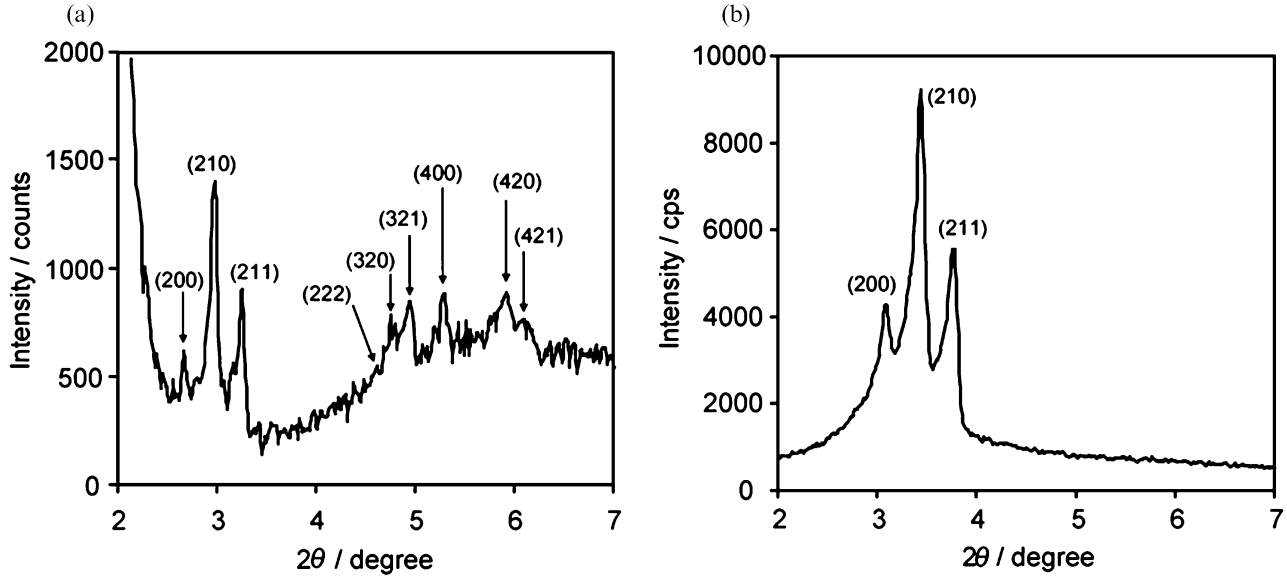

Figure 4. XRD patterns in the cubic phases of (a) **1**·**2** (1:5) at 120°C and (b) **1**·**3** (1:4) at 55°C.

micellar cubic mesophase with *Pm*3*n* symmetry with the lattice constant a_{cub}=57.3 Å.

Generation of micellar cubic mesophases

In a previous study, Lattermann and co-workers reported on the related covalent series of oligoamides having 3,4-dialkoxybenzoyl substituents (*46*). Micellar cubic mesophases were observed upon the elongation of the alkyl chains. This suggests that cubic mesophases occur with a subtle volume balance of the microsegregated polar amide groups and apolar alkyl chains. In the present study, complexes **1**·**2** and **1**·**3** exhibited micellar cubic mesophases. This is due to the lateral extension of alkyl chain volume in the acids because the

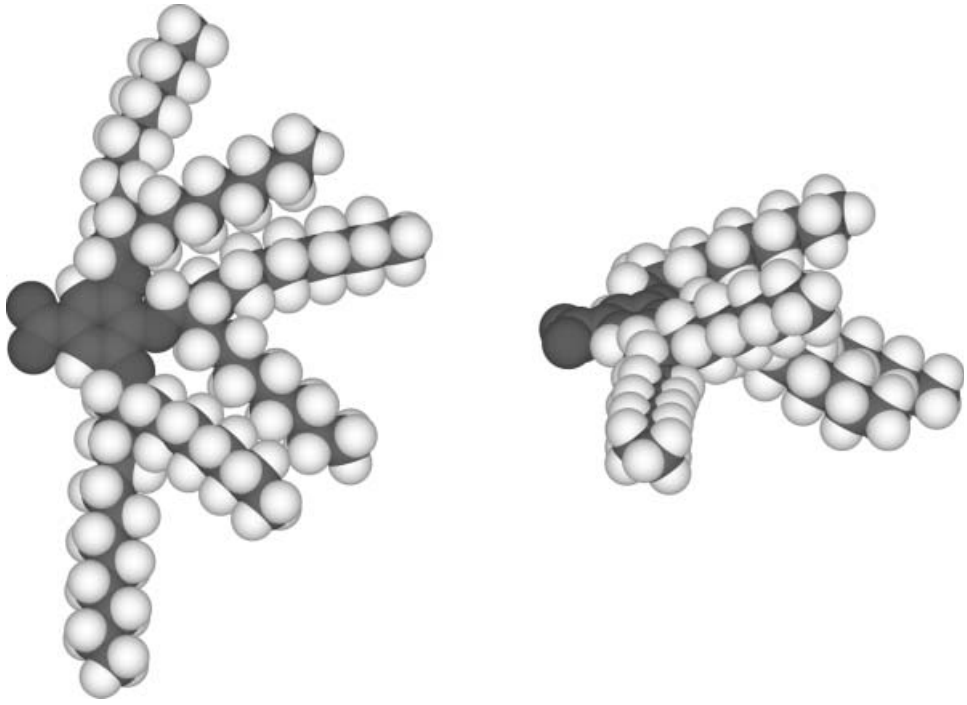

Figure 5. The molecular models of **3** generated by Chem3D: (a) top view; (b) side view.

analogous complexes with the normal alkyl chains exclusively exhibited hexagonal columnar mesophases despite the linear elongation of alkyl chains (*47*). For the acid with partially fluorinated alkyl chains (**2**), the cross-sectional area of a fluoroalkyl chain (ca. 30 $Å^2$) is larger than that of a normal alkyl chain (***ca.*** 20 $Å^2$) and an aromatic moiety (ca. 22 $Å^2$). In the case of the acid with branched alkyl chains (**3**), the laterally extended alkyl chains from the branching point provide an additional cross-sectional area of alkyl chains (Figure 5) compared to the analogous acid with normal dodecyl chains. Significant increase in interface curvature by laterally expanded chain volume could be responsible for the generation of the cubic mesophases. The interplay between ionic cohesive force at the core and the steric crowding at the peripheral chain shell upon increasing the molar ratio of the acids to **1** inhibited the formation of the stable infinite columnar aggregates. The generation of spheroidic aggregates occurs at a specific composite ratio for the most suitable chain volume appropriate to the formation of the micellar cubic mesophases.

4. Conclusion

We have demonstrated the morphological control of ionic liquid crystals by using ammonium carboxylates **1·2** and **1·3**. The chain volume in the resulting ionic complex introduced by the acid components was responsible for the generated mesophase morphologies and altered their thermal stabilities. In particular, the use of the benzoic acids bearing fluorinated or branched alkyl chains generated *Pm*3*n* micellar cubic mesophases. This is attributed to an increased interfacial curvature provided by the laterally expanded chain volume relative to the corresponding normal alkyl chain. It worth noting that the additional cross-sectional area of alkyl chain afforded by the branched alkyl chain was the key factor toward generation of the micellar cubic mesophase.

References

(1) Demus D., Goodby J.W., Gray G.W., Spiess H.-W., Vill V., Eds. *Handbook of Liquid Crystals*; Wiley-VCH: Weinheim, 1998.
(2) Kutsumizu S. *Curr. Opin. Solid St. Mater. Sci.* **2002**, *6*, 537–543.
(3) Impéror-Clerc M. *Curr. Opin. Colliod Interface Sci.* **2005**, *9*, 370–376.
(4) Ichihara M.; Suzuki A.; Hatsusaka K.; Ohta K. *Liq. Cryst.* **2007**, *34*, 555–567.
(5) Donnio B.; Heinrich B.; Gulik-Krzywicki T.; Delacroix H.; Guillon D.; Bruce D.W. *Chem. Mater.* **1997**, *9*, 2951–2965.
(6) Nishikawa E.; Samulski E.T. *Liq. Cryst.* **2000**, *27*, 1463–1471.
(7) Nishikawa E.; Yamamoto J.; Yokoyama H. *Chem. Lett.* **2001**, *30*, 454–455.
(8) Diele S. *Curr. Opin. Colloid Interface Sci.* **2002**, *7*, 333–342.
(9) Borisch K.; Diele S.; Göring P.; Kresse H.; Tschierske C. *J. Mater. Chem.* **1998**, *8*, 529–543.
(10) Percec V.; Holerca M.N.; Uchida S.; Cho W.-D.; Ungar G.; Lee Y.; Yeardley D.J.P. *Chem. Eur. J.* **2002**, *8*, 1106–1117.
(11) Seo S.-H.; Park J.-H.; Tew G.N.; Chang J.-Y. *Tetrahedron Lett.* **2007**, *48*, 6839–6844.
(12) Percec V.; Won B.C.; Peterca M.; Heiney P.A. *J. Am. Chem. Soc.* **2007**, *129*, 11265–11278.
(13) Cheng X.H.; Diele S.; Tschierske C. *Angew. Chem., Int. Ed.* **2000**, *39*, 592–595.
(14) Cheng X.; Das M.K.; Diele S.; Tschierske C. *Langmuir* **2002**, *18*, 6521–6529.
(15) Zhou X.; Narayanan T.; Li Q. *Liq. Cryst.* **2007**, *34*, 1243–1248.
(16) Fuchs P.; Tschierske C.; Raith K.; Das K.; Diele S. *Angew. Chem., Int. Ed.* **2002**, *41*, 628–631.
(17) Tschierske C. *J. Mater. Chem.* **2001**, *11*, 2647–2671.
(18) Kohlmeier A.; Janietz D. *Chem. Mater.* **2006**, *18*, 59–68.
(19) Vlad-Bubulak T.; Buchs J.; Kohlmeier A.; Bruma M.; Janietz D. *Chem. Mater.* **2007**, *19*, 4460–4466.
(20) Binnemans K. *Chem. Rev.* **2005**, *105*, 4148–4204.
(21) Ster D.; Baumeister U.; Chao J.L.; Tschierske C.; Israel G. *J. Mater. Chem.* **2007**, *17*, 3393–3400.
(22) Kouwer P.H.J.; Swager T.M. *J. Am. Chem. Soc.* **2007**, *129*, 14042–14052.
(23) Kim D.; Jon S.; Lee H.-K.; Back K.; Oh N.-K.; Zin W.-C.; Kim K. *Chem. Commun.* **2005**, 5509–5511.
(24) Ichikawa T.; Yoshio M.; Hamasaki A.; Mukai T.; Ohno H.; Kato T. *J. Am. Chem. Soc.* **2007**, *129*, 10662–10663.
(25) Marcos M.; Martín R.; Omenat A.; Barberá J.; Serrano J.L. *Chem. Mater.* **2006**, *18*, 1206–1212.
(26) Cook A.G.; Baumeister U.; Tschierske C. *J. Mater. Chem.* **2005**, *15*, 1708–1721.
(27) Ujiie S.; Yano Y.; Mori A. *Mol. Cryst. Liq. Cryst.* **2004**, *411*, 483–489.
(28) Ujiie S.; Mori A. *Mol. Cryst. Liq. Cryst.* **2005**, *437*, 25–31.
(29) Noguchi T.; Kishikawa K.; Kohmoto S. *Chem. Lett.* **2008**, *37*, 12–13.
(30) Noguchi T.; Kishikawa K.; Kohmoto S. *Bull. Chem. Soc. Japan* **2008**, *81*, 778–783.
(31) Percec V.; Glodde M.; Johansson G.; Balagurusamy V.S.K.; Heiney P.A. *Angew. Chem., Int. Ed.* **2003**, *42*, 4338–4342.
(32) Kohlmeier A.; Janietz D.; Diele S. *Chem. Mater.* **2006**, *18*, 1483–1489.
(33) Kohlmeier A.; Janietz D. *Liq. Cryst.* **2007**, *34*, 65–71.
(34) Terasawa N.; Monobe H.; Kiyohara K.; Shimizu Y. *Chem. Commun.* **2003**, 1678–1679.
(35) Alameddine B.; Aebischer O.F.; Amrein W.; Donnio B.; Deschenaux R.; Guillon D.; Savary C.; Scanu D.; Scheidegger O.; Jenny T.A. *Chem. Mater.* **2005**, *17*, 4798–4807.
(36) Johansson G.; Percec V.; Ungar G.; Zhou J.P. *Macromolecules* **1996**, *29*, 646–660.
(37) Kastler M.; Pisula W.; Wasserfallen D.; Pakula T.; Müllen K. *J. Am. Chem. Soc.* **2005**, *127*, 4286–4296.

(38) Meot-Ner M. *Chem. Rev.* **2005**, *105*, 213–284.
(39) Sada K.; Tani T.; Shinkai S. *Synlett* **2006**, *15*, 2364–2374.
(40) Lose D.; Diele S.; Pelzl G.; Dietzmann E.; Weissflog W. *Liq. Cryst.* **1998**, *24*, 707–717.
(41) Borisch K.; Diele S.; Göring P.; Kresse H.; Tschierske C. *Angew. Chem., Int. Ed.* **1997**, *36*, 2087–2089.
(42) Dukeson D.R.; Ungar G.; Balagurusamy V.S.K.; Percec V.; Johansson G.A.; Glodde M. *J. Am. Chem. Soc.* **2003**, *125*, 15974–15980.
(43) Kato T.; Matsuoka T.; Nishii M.; Kamikawa Y.; Kanie K.; Nishimura T.; Yashima E.; Ujiie S. *Angew. Chem., Int. Ed.* **2004**, *43*, 1969–1972.
(44) Bury I.; Heinrich B.; Bourgogne C.; Guillon D.; Donnio B. *Chem. Eur. J.* **2006**, *12*, 8396–8413.
(45) Zipp S.G.; Zipp A.P.; Madan S.K. *Coordination Chem. Rev.* **1974**, *14*, 29–45.
(46) Stebani U.; Lattermann G.; Festag R.; Wittenberg M.; Wendorff J.H. *J. Mater. Chem.* **1995**, *5*, 2247–2252.
(47) Katoh M.; Uehara S.; Kohmoto S.; Kishikawa K. *Chem. Lett.* **2006**, *35*, 322–323.